

Elastic Properties of Hard Sphere Crystals with Tripple (001) Nanolayer Inclusions within a Unit Supercell

J.W. Narojczyk^{1*}, K.W. Wojciechowski^{1,2}

¹ *Institute of Molecular Physics
Polish Academy of Sciences
ul. M. Smoluchowskiego 17, 60-179 Poznań, Poland
E-mail: narojczyk@ifmpan.poznan.pl

² *President Stanisław Wojciechowski University of Kalisz
Polytechnic Faculty
ul. Nowy Świat 4, 62-800 Kalisz, Poland*

Received: 18 November 2024; accepted: 2 December 2024; published online: 20 December 2024

Abstract: In this work, the recent studies on hard particle systems containing nanolayer inclusions are extended. Earlier studies showed that systems with nanolayer inclusion can be used to coarse- or fine-tune the auxetic properties of cubic crystals. Here, the impact of spatial distribution of individual inclusion layers on elastic properties of hard sphere crystal of cubic symmetry has been investigated by numerical simulations. The Monte Carlo method with Parinello-Rahman approach in NpT ensemble has been used to evaluate the elastic constants and Poisson's ratios for six different systems, each containing three nanolayers parallel to each other and orthogonal to $[001]$ -direction. The obtained results are compared with reference systems studied earlier. The studies have been performed for selected thermodynamic conditions. It has been shown that elastic properties weakly depend on the distribution of the inclusions within the structure if the inclusions are not formed by neighbouring layers. Some distributions of the inclusion layers change the period of the structure, which indicates that this factor does not have a big impact on the elastic properties. It is worth stressing that in a particular case the Poisson's ratio has been found to reach negative values in the $[111][1\bar{1}0]$ -directions which are not auxetic in cubic crystals.

Key words: auxetics, negative Poisson's ratio, nanolayers, hard spheres, nano-inclusions, Monte Carlo simulations

I. Introduction

When searching for a solution to a problem involving elastic properties of materials, one may often need materials with properties tailored for that particular problem. Unfortunately, to date, our ability to produce new materials upon request from the industry has been rather limited. The process is usually costly and time-consuming. The reason for this is that despite being one of the longest studied area of science, elastic properties of materials are far from being fully understood. The latter originate from interactions and phenomena that occur at the atomic level and despite our significant advancements in studying the world at nano-level, there is still a lot to be uncovered and understood. For this reason, it is important to study model crystalline structures, as they are the simplest systems describing the matter around us.

Poisson's ratio (PR) [1] is a common physical quantity that comes to mind when talking about elasticity of a material. In the simplest case, it describes how a particular material, subjected to longitudinal stretching load, elongates relatively to its transverse shrinkage. That was the case up to forty years ago, when people started to pay closer attention to systems for which PR could become negative. Within the scope of the above crude definition, it meant that the material could expand its transverse dimensions while being longitudinally stretched and, *vice versa*, transverse shrinkage could be observed under a longitudinal compression. The first mechanical models that exhibited such counter-intuitive behaviour were proposed in mid 1980s, independently by Almgreen [2] and Kolpakov [3]. Soon after the first man-made material exhibiting negative Poisson's ratio was made by Lakes [4] in late 1980s. In the same time, the first

thermodynamically stable model of a twodimensional elastically isotropic crystalline structure that showed negative Poisson's ratio was found [5] and rigorously solved [6] in the late 1980s by Wojciechowski. The work was later continued in [7, 8]. *Auxetics* [9], as negative Poisson's ratio materials are usually called today, due to the peculiar deformation mechanism, exhibit a number of characteristics that are useful from the point of view of practical applications [10–12], like enhanced stiffness, higher indentation resistance, fracture toughness, higher shear moduli and higher thermal impact resistance [11, 13], and others. Some materials can exhibit negative PR in some directions and positive or zero PR in others. Such materials were coined *partial auxetics* [14].

Since the discovery of negative Poisson's ratio materials, the intense studies [10, 12, 15–17] resulted in auxetic polymers [18, 19], composites [20, 21], and foams [22–25]. Auxetic properties have been also found or incorporated into nonwoven materials [26, 27] and fabrics [28–31]. Practical applications of these unusual properties of the new materials, although scarce, have been proposed to furniture industry [32, 33], medical sector [34–36] and others [37]. There is an abundance of ideas for practical applications of auxetics. However, obtaining an auxetic material is still not a trivial endeavour. In the late 1990s, Baughman *et al.* [38] explained the nature of auxetic properties found in cubic crystals. They showed that around 68% of cubic metals exhibit auxetic properties in some (narrow) range of crystallographic directions. This opened a possibility to enhance the already existing partial auxetic characteristics of materials instead of coping with a tedious process of designing new auxetics.

With the help of computer simulations, such studies can be performed relatively cheaply and efficiently. Using large supercomputers, one can study models of crystals and test modifications that could potentially lead to enhancement of the auxetic properties. To date, a number of such modifications introduced to crystalline structure have been studied [39–41]. It has been shown that introducing inclusions in the form of nanochannels [42, 43] not only can significantly decrease the values of the Poisson's ratio in the directions for which it is already negative, but also can induce new auxetic directions. The number of possible modifications that can be introduced into the crystals is limited only by our creativity. However, different modifications will exert different, sometimes unexpected results. While the mentioned nanochannel inclusions [43] significantly enhance auxeticity of the f.c.c. cubic crystal, an inclusion in the form of single nanolayer had only slightly decreased the Poisson's ratio of this crystal [44]. Moreover, the combined nanochannel nanolayer inclusion proved to entirely remove this inherent feature of cubic crystals, which are partial auxetic properties [45]. This shows that modifying a crystal structure in order to obtain required elastic properties, however effective, is not a simple task and requires further studies to get a broader understanding of how microscopic processes impact macroscopic properties. The most recent studies showed that such nanolayered systems (depending on the number of nanolayers introduced) can be used to coarse- [46] or fine-tune [47] the auxetic properties of cubic crystals. In this work, the studies of systems with nanolayer inclusions are further extended to

investigate how the spatial ordering of individual nanolayers will impact elastic properties of the model. This subject is timely and relevant, as the recent advancements in nanotechnology will allow, possibly in the near future, the creation of such systems [48].

The article has the following structure. In Sec. II, the studied model is described. In Sec. III, elementary information about research methodology is provided. Sec. IV presents the results and their discussion. The summary and conclusions are placed in Sec. V.

II. The Model

In this work, models of hard spheres are considered. The spheres interact with a purely geometrical interaction that can be described in the following form:

$$\frac{u_{ij}}{k_B T} = \begin{cases} \infty, & r_{ij} < \sigma_{ij}, \\ 0, & r_{ij} \geq \sigma_{ij}, \end{cases} \quad (1)$$

where r_{ij} is the distance between the centres of spheres i and j , $\sigma_{ij} = (\sigma_i + \sigma_j)/2$, σ_i , and σ_j are the diameters of spheres i and j . The *hard sphere* (HS) potential is a very simple but non-trivial interaction. It very well mimics short-range correlations that originate from the excluded volume effects [49–51]. For this reason, it and its generalizations to non-spherical particles constitute one of the fundamental interactions used in the condensed matter physics [50] and theory of liquids [52]. Despite its simplicity, the hard sphere system exhibits melting and auxeticity. Thus, it can be used to study auxetic properties, as the f.c.c. hard sphere crystal is partially auxetic [53].

The models considered in this article are based on the f.c.c. crystals of N hard spheres, each with the diameter of σ . The crystal has been modified by the replacement of some of the spheres ($N_{\text{inc}} < N$) with spheres of another diameter $\sigma' \neq \sigma$. The replaced spheres can be thought of as an *inclusion* of different particles into the *matrix* crystal. In general, there are many possible ways to arrange this replacement. In this article, we have focused on arranging these inclusions in the form of (001)-layers orthogonal to [001]-direction. In each of the studied models, three layers are selected to constitute the inclusions in the unit supercell formed by $6 \times 6 \times 6$ unit cells. This indicates that $N_{\text{inc}} = 3 \cdot 2xy$ and the ratio $c = N_{\text{inc}}/N$, regarded as the *concentration* of inclusion particles, is equal to $3/(2z)$, where x , y , and z are the number of f.c.c. unit cells in the respective directions. The primary (non-inclusion) spheres will be referred to as the *matrix* spheres. The changes of the elastic properties of proposed models have been studied with respect to different values of inclusion sphere diameters, thus the *scaling factor* $s = \sigma'/\sigma$ is introduced. The systems have been studied under different thermodynamic conditions, i.e. different values of the reduced pressure, defined as $p^* = \beta\sigma^3 p$, where $\beta = (k_B T)^{-1}$ and p is the pressure. The models have been considered in periodic boundary conditions. Thus, effectively one obtains systems with periodic stacks of parallel inclusion layers. For model samples where $z > 4$, there is an

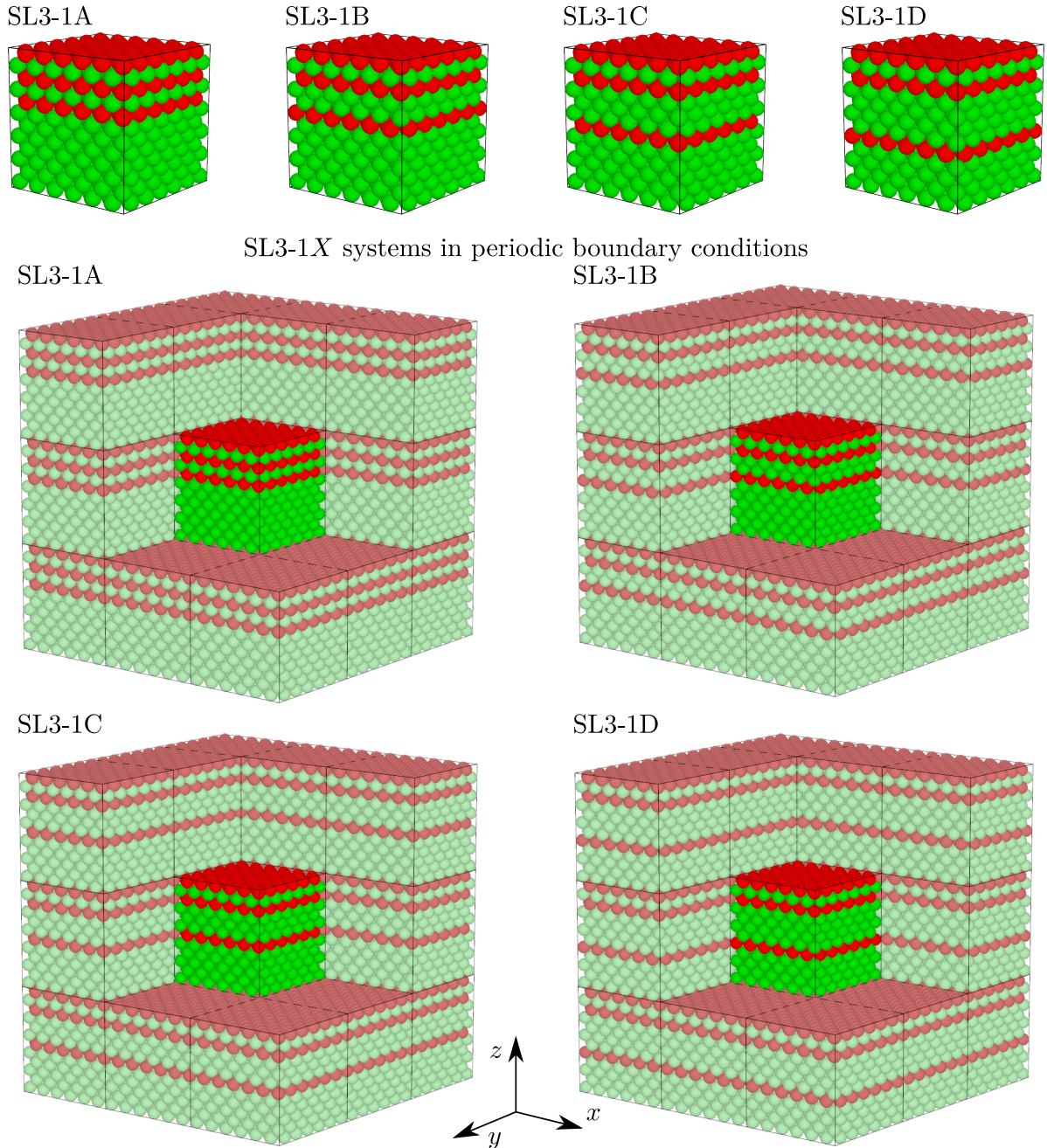


Fig. 1. Visualization of studied systems containing three inclusion layers orthogonal to $[001]$ -direction. The presented systems contain a single layer of matrix crystal between the first and second inclusion layer, and vary in the number of matrix layers between the second and third inclusion layer. The bottom part presents these systems in periodic boundary conditions (part of the periodic images has been removed to facilitate the view)

increasing number of possibilities how the three inclusion layers can be distributed along the z axis. In previous studies [46], the increasing number of inclusion layers within the sample, as well as the decrease of the period of the structure, were the two main factors, whose impact on the elastic properties has been investigated. The concentration c of those systems changed from $1/6$ to $1/2$. Here, for the fixed $c = 1/4$ the impact of different ordering of inclusion layer

along with the *fixed* period of the structure, on elastic properties (and in particular the Poisson's ratio) is being investigated. In [46] two categories of structures were considered, one where the inclusions occupied the neighbouring crystallographic layers (NL system) and the second, where the inclusion layers have been separated (SL) by a number of layers of matrix particles. Here we consider another two sets of models, which are variants of the SL systems. Namely, when

the two out of three inclusion layers are separated by one (category 1) or by two (category 2) matrix layers. The third inclusion layer is distanced from the former two by varying number of matrix layers, thus forming four different systems of category 1 and two different systems from category 2. Since the considered models are based on SL3 system from [46], they will be referenced respectively as SL3-1X and SL3-2Y, where $X = A, B, C, D$ and $Y = A, B$. These six models cover all non-equivalent inclusion layer ordering for systems in which (i) all inclusion layers are separated, (ii) two of the inclusions are separated either by one or two matrix layers and (iii) $z = 6$ f.c.c. cells. The volume of space occupied by each model is designated by a parallelepiped described by the matrix \mathbf{h} . A symmetric matrix, defined by vectors that constitute the edges of the parallelepiped. This matrix will be further referenced to as the *box matrix*. Visualization of studied systems is presented in Figs. 1 and 2.

III. The Method

The free enthalpy change that corresponds to a thermodynamically reversible system that is subjected to an external pressure p can be expressed in the following form [49]:

$$\Delta G = \frac{V_p}{2} \sum_{ijkl} B_{ijkl} \varepsilon_{ij} \varepsilon_{kl}, \quad (2)$$

where B_{ijkl} are the components of the fourth rank elastic tensor of elastic constants, ε_{ij} are the components of the Lagrange strain tensor, V_p is the volume of the system at equilibrium at pressure p , and i, j, k, l correspond to x, y, z .

To calculate elastic properties for the described models, the Monte Carlo (MC) computer simulations based on the concept by Parrinello and Rahman [54, 55] were used. The simulations were performed in the isobaric-isothermal ensemble (NpT) [7, 49], i.e. for a fixed number of particles, and under constant pressure and temperature. The choice of the method was governed by the fact that it gives the possibility to calculate the complete elastic compliance tensor of components $S_{\alpha\beta\gamma\delta}$. The 21 independent components of the fourth-rank tensor $S_{\alpha\beta\gamma\delta}$ are obtained from the shape fluctuations of the periodic box, which can be directly obtained from the strain tensor ε – a second-rank, symmetric tensor. For a system under the pressure p , this relation reads [49, 55]:

$$\varepsilon = \frac{1}{2} (\mathbf{h}_p^{-1} \cdot \mathbf{h} \cdot \mathbf{h}_p^{-1} - \mathbf{I}). \quad (3)$$

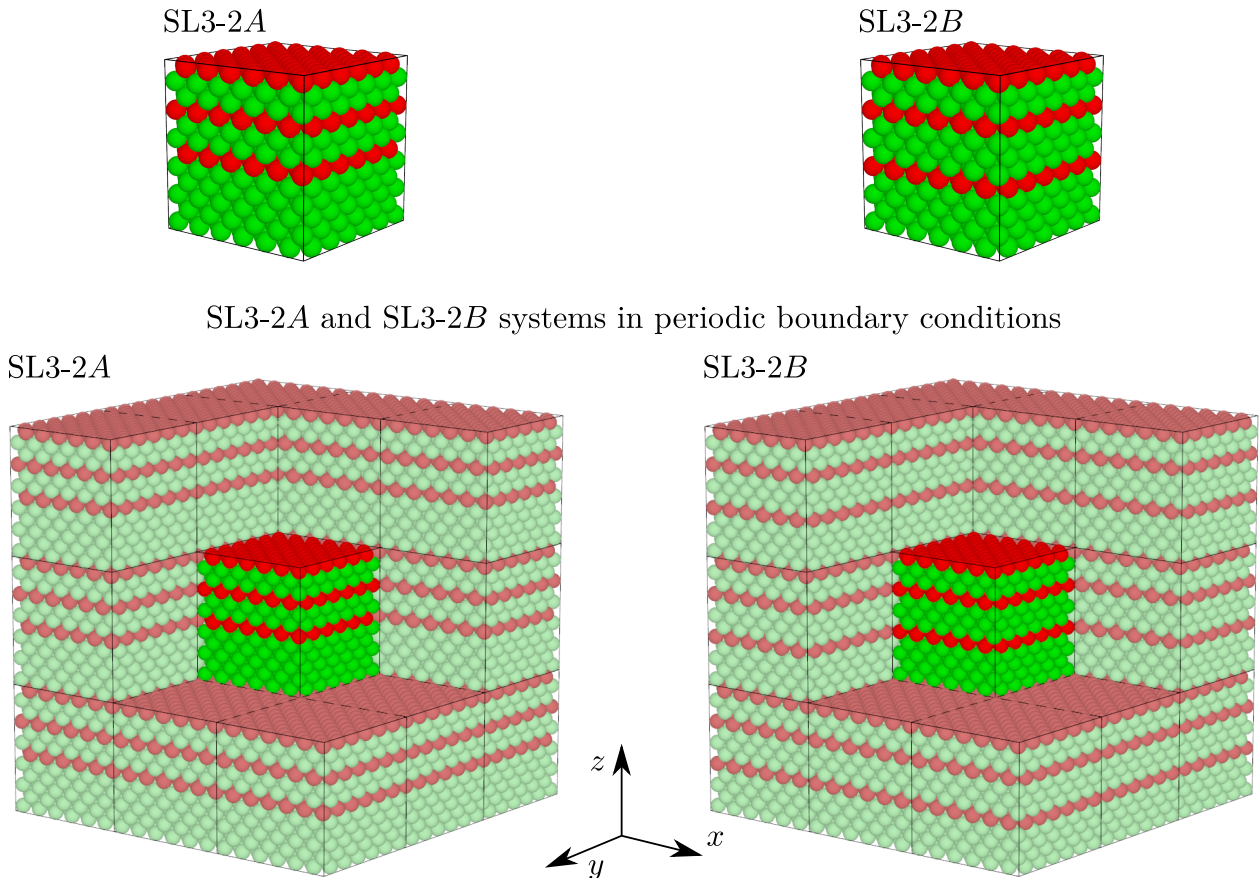


Fig. 2. Visualization of studied systems containing three inclusion layers oriented orthogonally to [001]-direction. The presented systems contain a double layer of matrix crystal between the first and second inclusion layer, and vary in the number of matrix layers between the second and third inclusion layer. The bottom part presents these systems in periodic boundary conditions (part of the periodic images has been removed to facilitate the view)

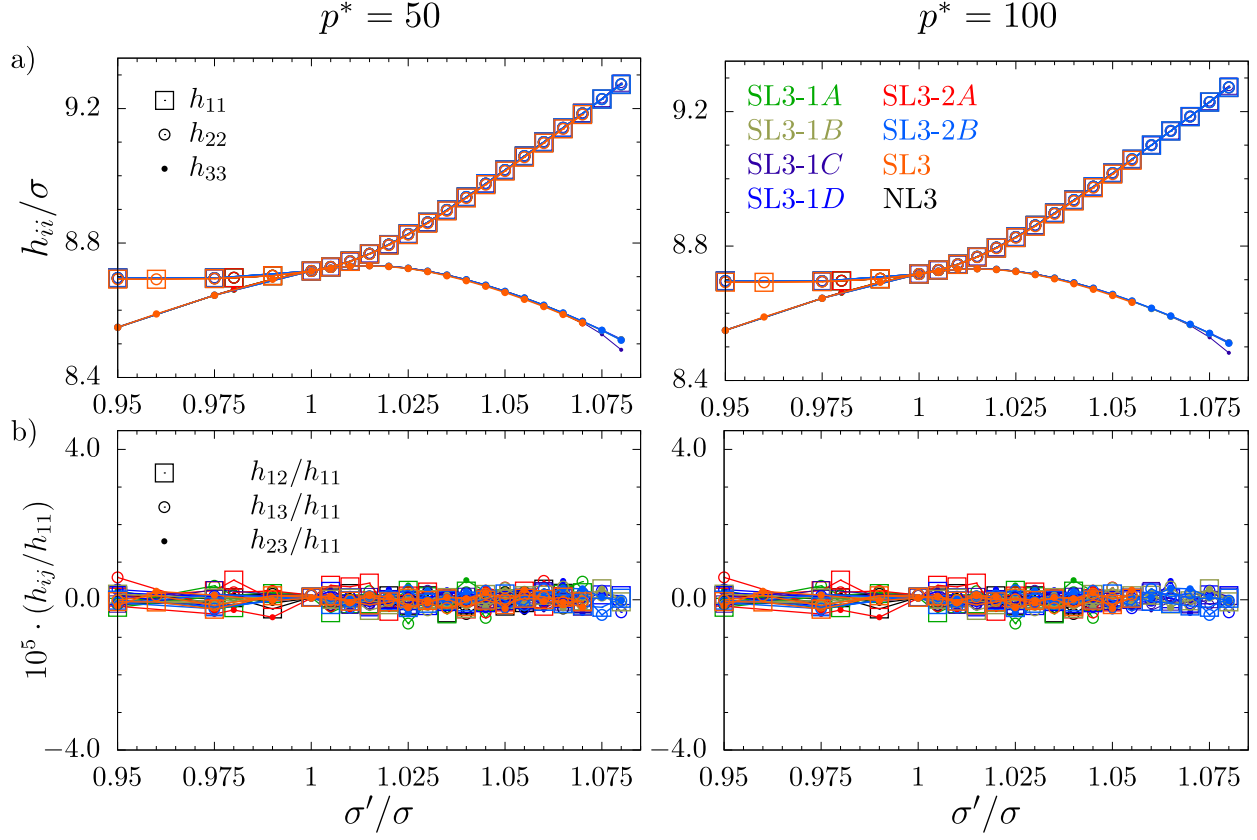


Fig. 3. The elements of the box matrix \mathbf{h} for studied models, composed over the data for reference models studied in [46], arranged in columns for both studied values of pressure. In the row a) the diagonal box matrix elements are presented. In the row b) the ratio of the off-diagonal elements and h_{11} , scaled by 10^5

For simplicity, in the calculations we use the reduced pressure defined as $p^* = p\beta\sigma^3$. In eq. (3), \mathbf{I} is the unit matrix of the dimensionality three and $\mathbf{h}_p \equiv \langle \mathbf{h} \rangle$ is the reference box matrix, i.e., the average box matrix at equilibrium under (dimensionless) pressure p^* . One of the many advantages of this approach is the ability of the system to optimize its shape under arbitrarily applied thermodynamic conditions. Moreover, the symmetry of the box matrix allows one to avoid deformations that would result only in rotation of the system. The latter are irrelevant to the calculation of elastic properties. The expression that allows one for computing components of the elastic compliance tensor $S_{\alpha\beta\gamma\delta}$ from the elastic strain tensor has the following form [49]:

$$S_{\alpha\beta\gamma\delta} = \beta V_p \langle \Delta \varepsilon_{\alpha\beta} \Delta \varepsilon_{\gamma\delta} \rangle, \quad (4)$$

where $V_p = |\det(\mathbf{h}_p)|$ is the average volume of the system at equilibrium, under pressure p^* , $\Delta \varepsilon_{\alpha\beta} = \varepsilon_{\alpha\beta} - \langle \varepsilon_{\alpha\beta} \rangle$, and $\langle \varepsilon_{\alpha\beta} \rangle$ is the ensemble average. The Greek indices $\alpha, \beta, \gamma, \delta$ indicate directions x, y, z in the Cartesian coordinate system. The elastic constants tensor components B_{ijkl} are related to the elastic compliance tensor components S_{ijkl} by the equation [56]:

$$\sum_{n,m} S_{ijmn} B_{mnkl} = \frac{1}{2} (\delta_{ik} \delta_{jl} + \delta_{il} \delta_{jk}), \quad (5)$$

where δ_{ij} is the Kronecker delta. The general relation between the components $S_{\alpha\beta\gamma\delta}$ of the elastic compliance tensor and the Poisson's ratio can be expressed in the following form [57]:

$$\nu_{nm} = -\frac{m_\alpha m_\beta S_{\alpha\beta\gamma\delta} n_\gamma n_\delta}{n_\zeta n_\eta S_{\zeta\eta\kappa\lambda} n_\kappa n_\lambda}. \quad (6)$$

This formula allows one to calculate the Poisson's ratio for any pair of mutually orthogonal directions \vec{n} and \vec{m} which, respectively, are the loading direction and the transverse direction of PR measurement. The n_i and m_j are their respective direction cosines. It should be noted that the Einstein summation convention is used on Greek indexes and, for the sake of clarity, in the remaining part of the manuscript we express the $S_{\alpha\beta\gamma\delta}$ tensor elements with the elastic compliance matrix S_{ij} elements using the Voigt representation [58]. The same holds for the components of the elastic constants tensor $B_{\alpha\beta\gamma\delta}$. The Latin indices for the S_{ij} and B_{ij} elements of those symmetric square matrices take the values $i, j = 1, \dots, 6$. As a final remark, it should be stressed that the approach, to calculate elastic properties, described here concerns infinitesimally small deformations (strains). Further details on the calculation of the elastic properties using this method are given in the reference [49].

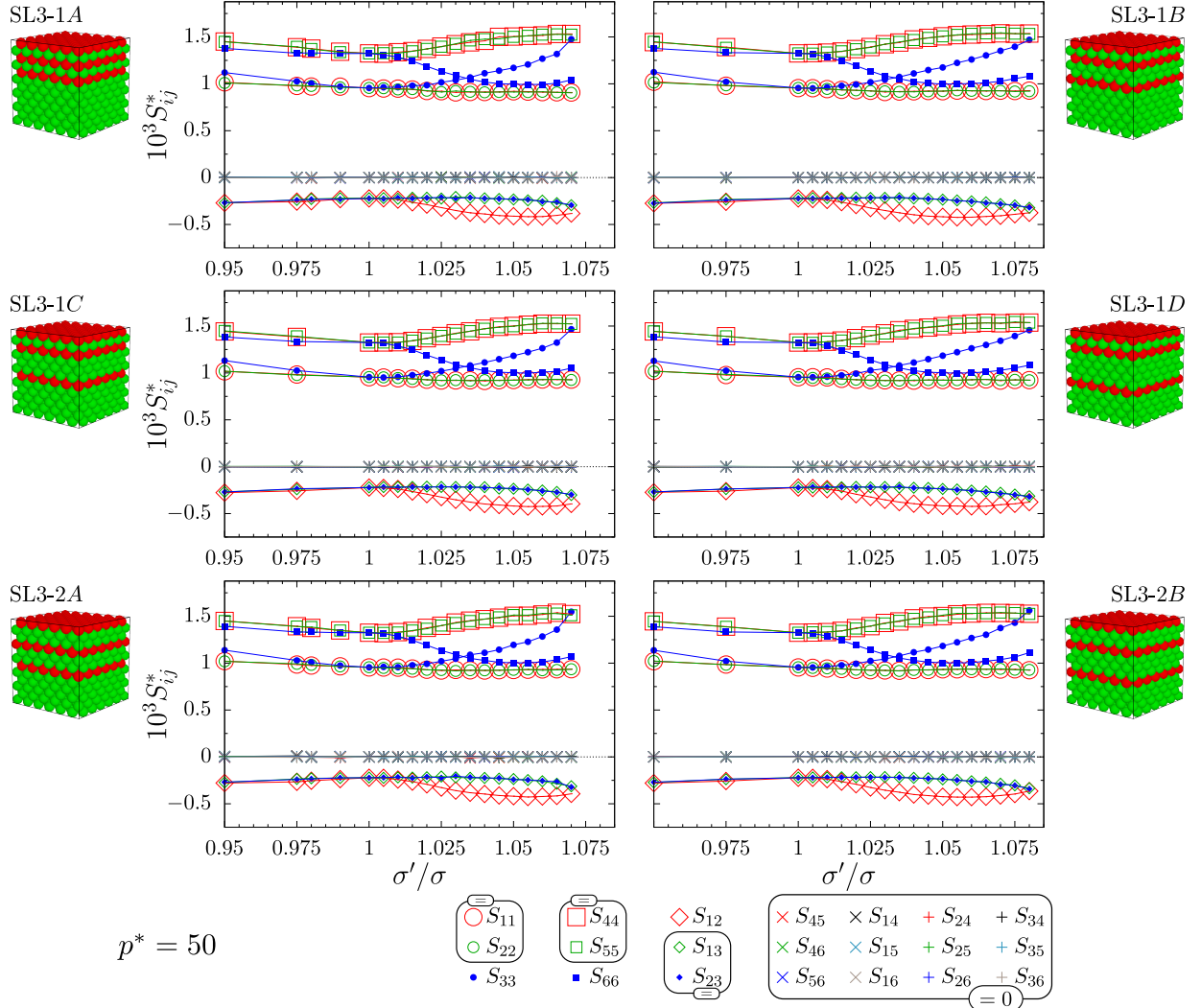


Fig. 4. The elastic compliance matrix elements $S_{ij}^* = S_{ij}\beta\sigma^3$ for the six models studied in this work at $p^* = 50$, plotted with respect to σ'/σ

III. 1. Computational Details

Elastic properties of the models have been obtained with the use of MC simulations carried out in the NpT ensemble. To study different thermodynamic conditions, the pressure has been changed. The models were subjected to two different values of external (reduced) pressure $p^* = 50$ and 100. In order to increase the efficiency of simulations, the lowest pressure has been selected such as to avoid diffusion of particles within the crystal structure. The size of the simulated samples was $N = 864$, which corresponds to $6 \times 6 \times 6$ f.c.c. unit cells. The number of particles forming inclusions was $N_{\text{inc}} = N/4 = 216$, which corresponds to the concentration $c = 25\%$. Since the interaction potential used in this work is purely geometrical in nature, any changes to the elastic properties can be observed only when the geometry of the interacting particles changes. Thus, for each model and each value of p^* , the diameters of the inclusion particles σ' were changed with respect to diameters of matrix particles (σ). The number of different values for scaling factor σ'/σ was

selected from the range of 0.95 to 1.08. The results were averaged over at least seventy independent runs for each set of parameters and for each model. The following section discusses only the results obtained for stable systems. Thus, the presented range of σ'/σ for individual models and thermodynamic conditions differs. Each simulation run took 10^7 MC cycles. The first 10^6 of which was treated as the period when the system reached thermodynamic equilibrium, and was removed from calculations.

IV. Results and Discussion

It has been shown that introducing one [44] or more [46, 47] nanolayer inclusions in parallel to each other and orthogonal to [001]-direction, induces the change of the shape of the system from cubic to cuboid. The ordering of layers inside the supercell is not relevant, which is shown in Fig. 3, where the box matrix elements for all the studied systems

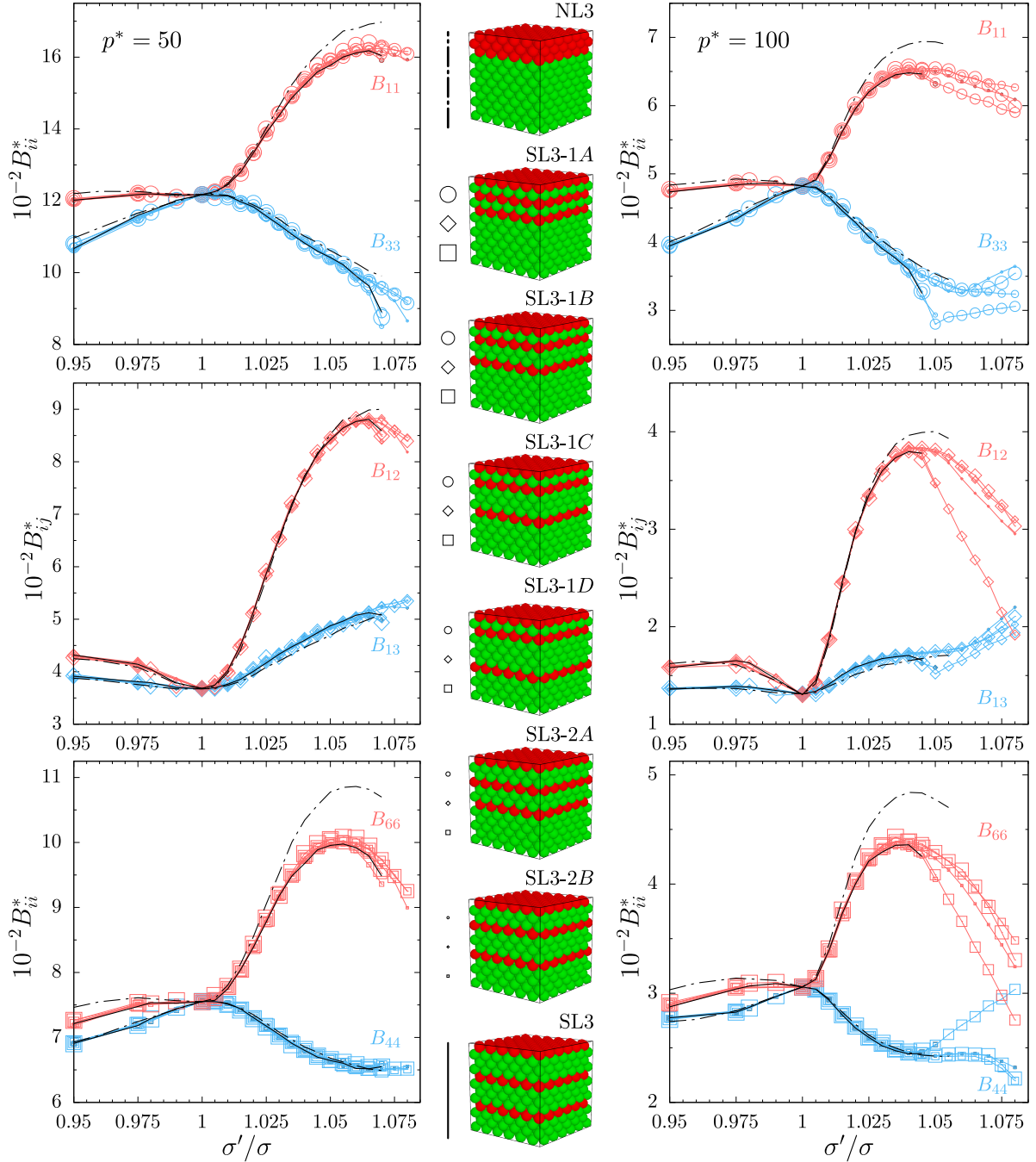


Fig. 5. The non-zero elastic constants $B_{ij}^* = B_{ij}\beta\sigma^3$, compared for all the studied models. The respective constants have been pair-wise, grouping together constants that are equivalent in the cubic symmetry: B_{11} and B_{33} , B_{12} and B_{13} , B_{44} and B_{66} are plotted in respective rows. The plots have been arranged in columns for different pressure values $p^* = 50$ (left) and $p^* = 100$ (right). Black lines designate data for the reference SL3 (solid) and NL3 (dash-dot) systems

have been presented and compared with the previously studied NL3 and SL3 [46] models. It can be seen that with the increase of the inclusion particle diameters (σ'), the systems expand in x - y plane (increase of h_{11} and h_{22}), and due to an excess volume between matrix particles they compress along z -direction, which is reflected in the decrease of h_{33} . On the other hand, when $\sigma'/\sigma < 1$ the systems are com-

pressed in the direction orthogonal to the inclusion planes, but no noticeable change in h_{11} and h_{22} is observed. This is due to the matrix crystal not being able to compress further. In part (b) of Fig. 3 one can observe the off-diagonal elements of the box matrices for all the studied system, plotted in relation to h_{11} . As it can be seen, they are at least five order of magnitude less than their diagonal counterparts,

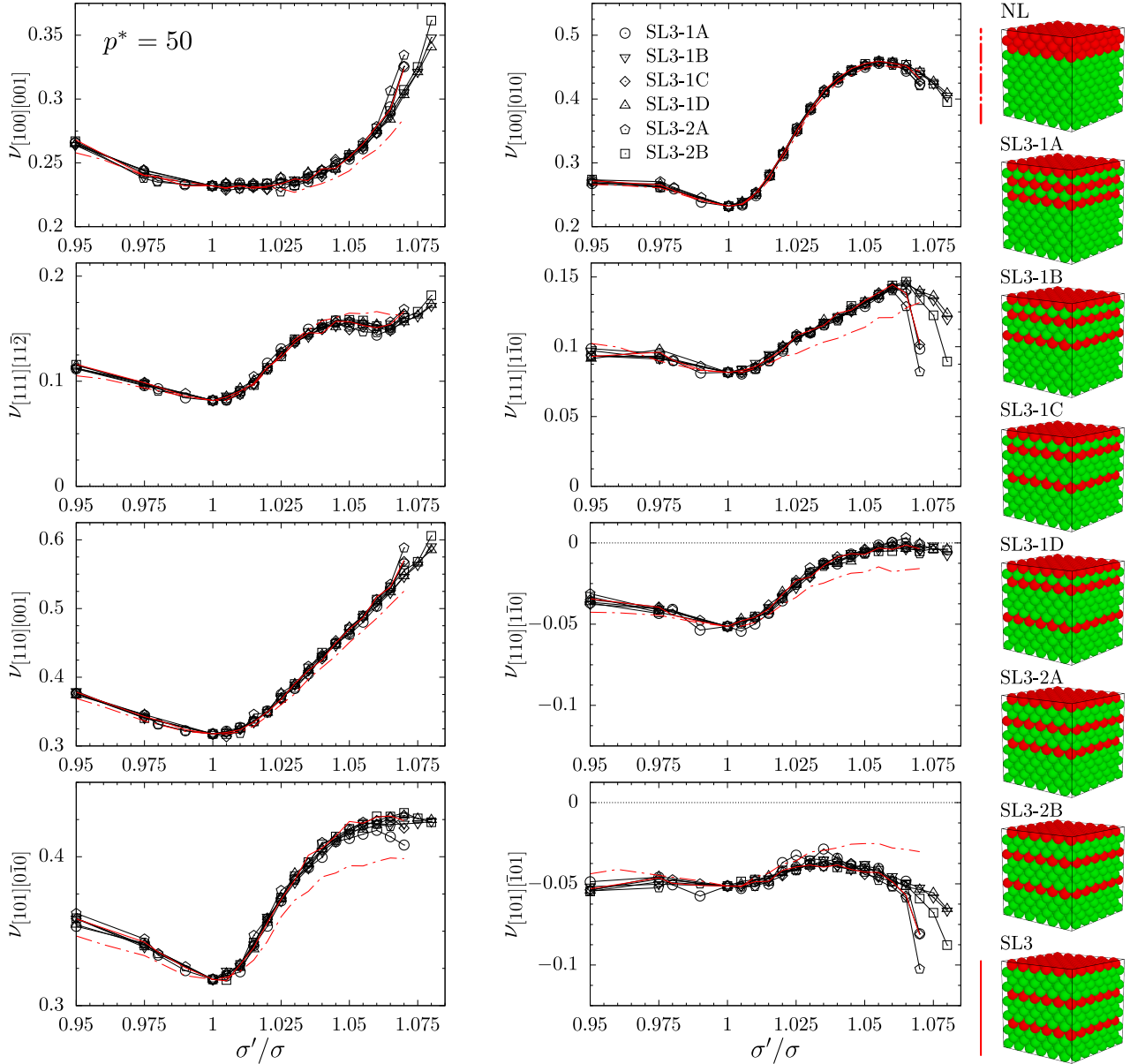


Fig. 6. Poisson's ratio in main crystallographic directions for all studied systems at $p^* = 50$, compared to NL3 and SL3 reference systems

thus they can be treated as zero. This shows that inclusions indeed transformed our models into cuboid systems, which definitely leads to changes in the symmetry of studied model crystals.

To investigate the symmetry of the structure, components of the elastic compliance matrices for all the SL3-1X and SL3-2Y systems have been plotted with respect to σ'/σ . It should be noted that the introduction of the (001) inclusion layers into the crystal of cubic symmetry, one loses the 4-fold symmetry axis for the in-plane directions (x , y in this case). Different arrangement of individual inclusions within the supercell lower the symmetry to 2-fold axis in [100] and [010] directions for SL3-1A, SL3-1D, SL3-2A, as well as both NL3 and SL3 reference systems. However, in the case of remaining SL3-1B, SL3-1C, and SL3-2B sys-

tems this is only 1-fold symmetry axis in the respective directions. In Fig. 4, it can be observed that with the increase of σ'/σ the components of elastic compliance matrix change such that the conditions for the tetragonal symmetry are fulfilled [58]: $S_{11} = S_{22}$, $S_{44} = S_{55}$, $S_{13} = S_{23}$, and $S_{ij} = 0$ for: $i = 1, \dots, 5$, $j = 4, 5, 6$, $i \neq j$. Thus, the elastic compliance matrix has the following form:

$$\mathbf{S} = \begin{bmatrix} S_{11} & S_{12} & S_{23} & 0 & 0 & 0 \\ \cdot & S_{11} & S_{23} & 0 & 0 & 0 \\ \cdot & \cdot & S_{33} & 0 & 0 & 0 \\ \cdot & \cdot & \cdot & S_{44} & 0 & 0 \\ \cdot & \cdot & \cdot & \cdot & S_{44} & 0 \\ \cdot & \cdot & \cdot & \cdot & \cdot & S_{66} \end{bmatrix}. \quad (7)$$

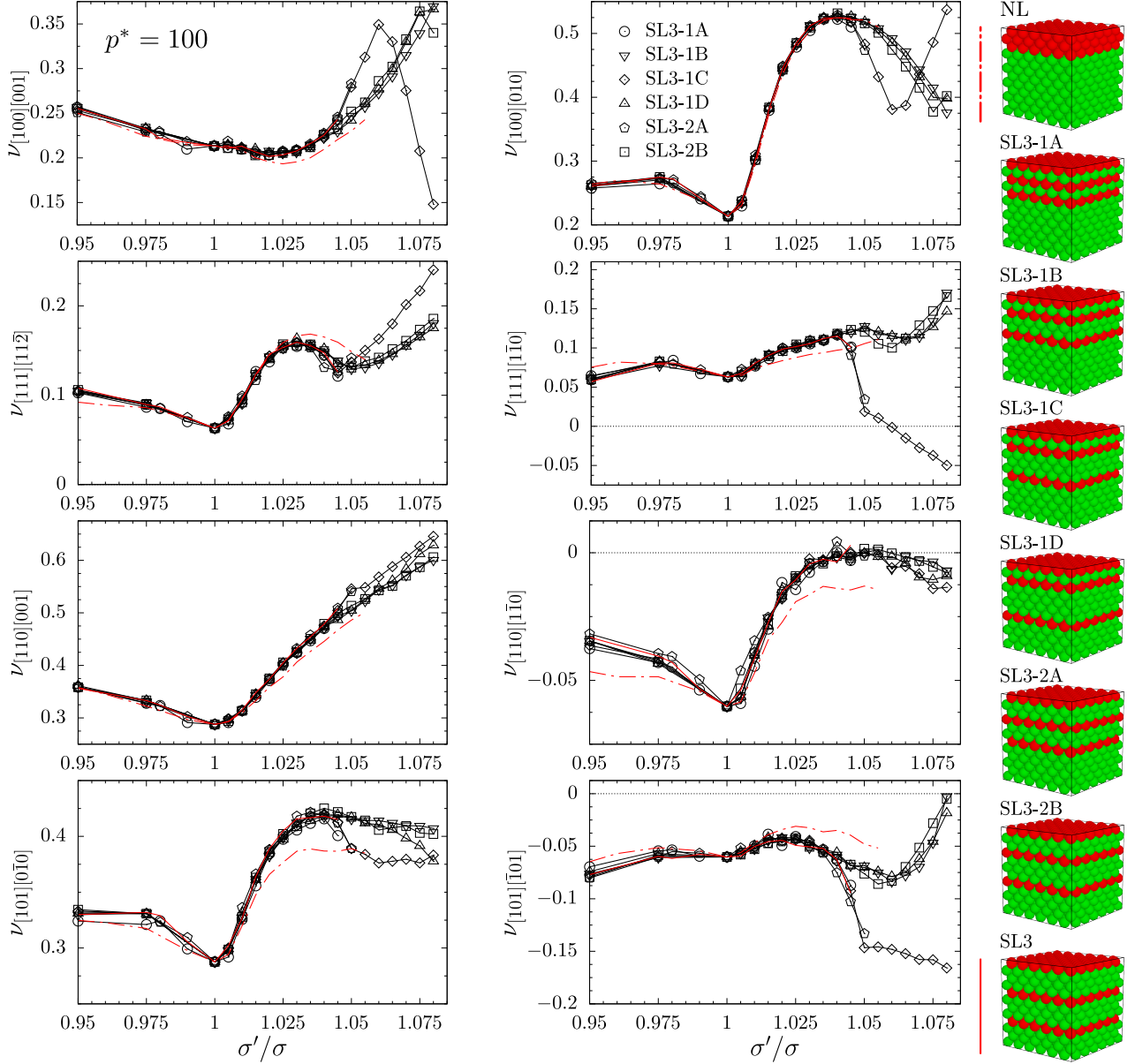


Fig. 7. Poisson's ratio in main crystallographic directions for all studied systems at $p^* = 100$, compared to NL3 and SL3 reference systems

Although only small changes in elastic compliances are observed when $\sigma'/\sigma < 1$, one should note that for every case when $\sigma'/\sigma \neq 1$ the system loses cubic symmetry and exhibits tetragonal symmetry [58].

In Fig. 5, the comparison of the elastic constants for the studied models has been presented. From eq. (5) one can see that elastic constants matrix \mathbf{B} can be obtained by inverting the elastic compliance matrix \mathbf{S} and, in the result, the former will have the form:

$$\mathbf{B} = \begin{bmatrix} B_{11} & B_{12} & B_{23} & 0 & 0 & 0 \\ \cdot & B_{11} & B_{23} & 0 & 0 & 0 \\ \cdot & \cdot & B_{33} & 0 & 0 & 0 \\ \cdot & \cdot & \cdot & B_{44} & 0 & 0 \\ \cdot & \cdot & \cdot & \cdot & B_{44} & 0 \\ \cdot & \cdot & \cdot & \cdot & \cdot & B_{66} \end{bmatrix}. \quad (8)$$

The data in Fig. 5 has been compared in pairs of constants which are equivalent in the case of cubic symmetry, namely: B_{11} and B_{33} , B_{12} and B_{13} , B_{44} and B_{66} are arranged in rows. Open symbols of different size designate respective models studied in this work. The data has been additionally compared against the reference systems NL3 and SL3 indicated by dash-dot and solid black curves, respectively. The columns indicate different pressure values set in the simulations. The differences between NL3 and SL3 systems (discussed in [46]) are especially apparent for B_{11} and B_{66} constants. One can notice that results for SL3-1X and SL3-2Y systems are closer to SL3 system and their relation to σ'/σ weakly depends on the type of the system, i.e. the arrangement of the individual layers. One exception is the SL3-1C system, which (at $p^* = 100$) clearly deviates from

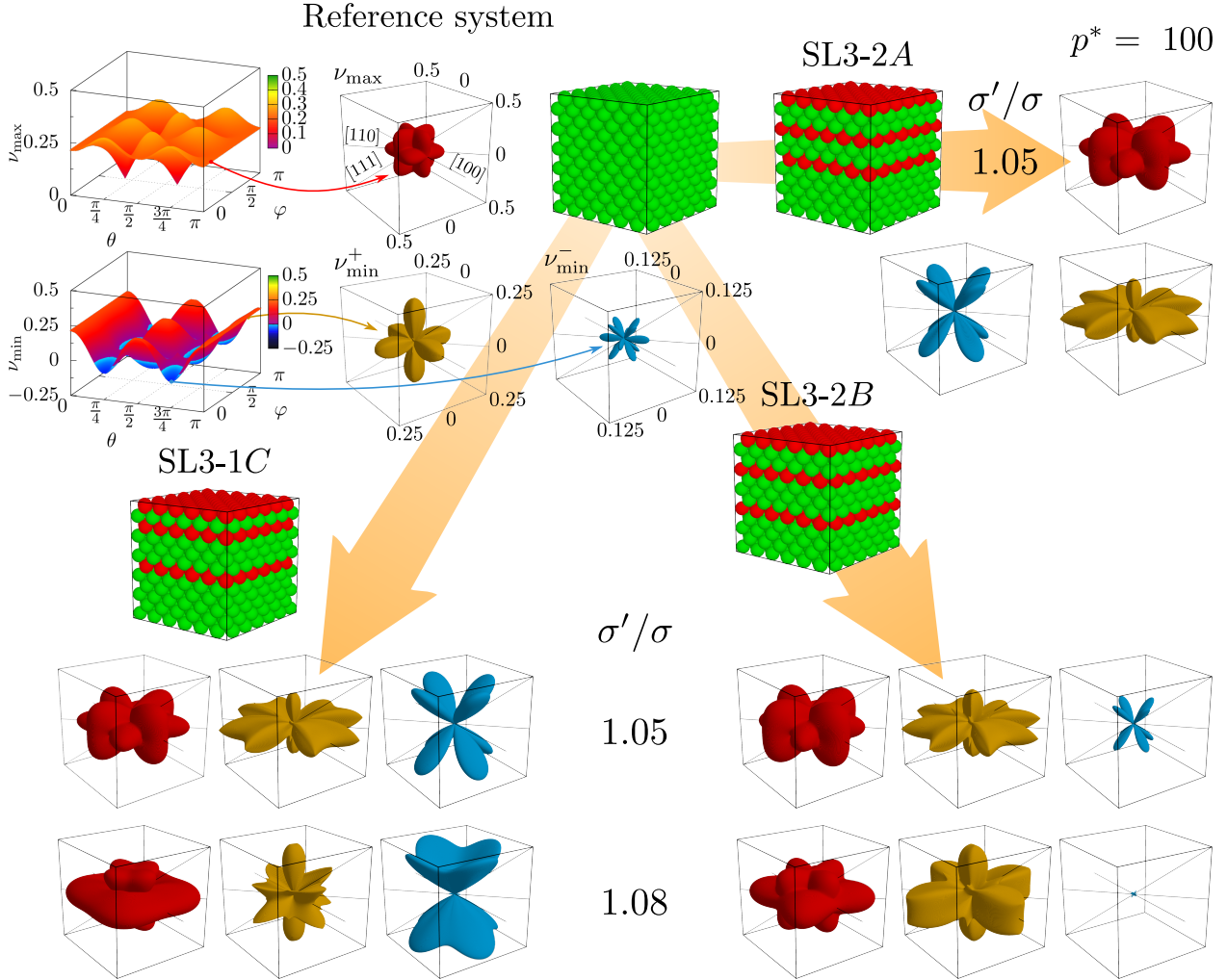


Fig. 8. The surfaces of Poisson's ratio for selected systems at pressure $p^* = 100$. The surfaces have been plotted in spherical coordinates (ν_{\max} – red, positive part of ν_{\min}^+ – yellow, negative part of ν_{\min}^- – blue), as shown for the reference system at $\sigma'/\sigma = 1$. The scale for each respective cube is indicated at the plots for the reference system

the other studied models. It is worth noting that this is one of the models that does not exhibit the 2-fold symmetry axis in $[100]$ and $[010]$ directions. Furthermore, the dependence of elastic constants on σ'/σ for SL3-1C model is not monotonic, which might suggest a possible phase transition around $\sigma'/\sigma = 1.05$.

Figs. 6 and 7 present Poisson's ratio calculated in the main crystallographic directions $[100]$, $[110]$, and $[111]$ for systems under the reduced pressure p^* equal to 50 and 100, respectively. The directions $[100]$ and $[111]$ in the cubic symmetry are the co-called high symmetry directions, namely the value of the Poisson's ratio does not depend on the choice of the direction of measurement (\vec{m}). It can be seen in the figures that this is not the case for the tetragonal symmetry. Moreover, the directions $[110]$ and $[101]$, equivalent in cubic case, are different in the presented systems. Poisson's ratio values in the $[110][\bar{1}\bar{1}0]$ -direction, which is auxetic in cubic case ($\sigma'/\sigma = 1$), tend to zero along with the increase of inclusion particle diameters. There is very small or zero aux-

eticity in this direction at high σ'/σ for both pressures. In the current case at $p^* = 50$, the PR in this direction is close to -0.1 for systems SL3-1A, SL3-1C, SL3-2B, and SL3-2A – for which it is the lowest, and close to -0.061 for the remaining models. For both pressures, the Poisson's ratio for the studied systems is varying only in some cases at the highest considered σ'/σ . In general, the PR values among the studied models are very close to each other for the given σ' . They are also close to the SL3-1X reference system, which suggests that spatial localization of the individual layers inside the crystal has a rather small effect, provided that the individual layers are separated with at least one layer of particles forming the matrix crystal. A similar pattern can be observed for systems under the pressure $p^* = 100$ (Fig. 7). However, here we can observe that the system SL3-1C behaves differently from the other ones. One can see that auxeticity is induced in the $[111][\bar{1}\bar{1}0]$ direction, and the PR values in the $[101][\bar{1}01]$ -direction are significantly lower, reaching $\nu = -0.162$. Similarly to the above discussion of B_{ij}

elastic constants for SL3-1C system, here one can see that the behaviour of Poisson's ratio versus σ'/σ is not monotonic, which might suggest the possible phase transition in the vicinity of $\sigma'/\sigma = 1.05$. However, confirming this will require further in-depth studies of SL3-1A, SL3-1C, SL3-2A, and possibly the SL3 systems (as they show tendency to decrease the value of PR in this direction). This will be the subject of a future article.

Fig. 8 shows 3D visualizations of Poisson's ratio in spherical coordinates for selected systems. The data presented in the inserts are the surfaces of maximum and minimum Poisson's ratios plotted with respect to the loading direction \vec{n} parametrized by polar and azimuthal angles θ , φ . To facilitate the comparison of the data between different systems, these surfaces have been plotted in a spherical coordinate system, forming a set of three distinct plots per given system and particular value of σ'/σ . The red plot corresponds to the surface of maximum PR (ν_{\max}^+), the yellow and blue plots correspond to positive (ν_{\min}^+) and negative (ν_{\min}^-) parts of the minimum PR surface, respectively. The respective inserts have been plotted to the same scale, indicated on the reference system. Here one can see the reason for the different behaviour of SL3-1C and SL3-2B systems in Fig. 7. It can be observed that whereas for $\sigma'/\sigma = 1.05$ all the systems have similar elastic properties (notably the auxeticity of SL3-2B is smaller), for $\sigma'/\sigma = 1.08$ the auxeticity of SL3-2B has been almost removed and for SL3-1C the latter has been significantly enhanced.

V. Conclusions

In this work, a number of hard particle systems containing three nanolayer inclusions in the unit supercell have been investigated. The systems differed in spatial localisation of individual nanolayers, which were parallel to each other and oriented orthogonally to [001] direction. The investigations have been carried out using Monte Carlo computer simulations in the isothermal-isobaric ensemble, based on the idea by Parrinello and Rahman. The investigations, supported by reference models from previous studies, showed that the most notable differences in elastic properties of such models are observed in cases where the introduced inclusions are either grouped together or they are separated by at least one layer of the matrix crystal. Elastic properties of different variants of systems with separated inclusions have been found to be very close. This suggests that in practical realisation of such systems using modern nanotechnology [48], the strict control over depositing individual layers may not be a critical factor in achieving a system with desired elastic properties. An important note should be made at the end. Namely, in the case of some of the studied systems a decrease of the Poisson's ratio has been observed, and in one of the systems *new auxetic directions* have been induced.

Acknowledgment

This work was supported by the grant No. 2017/27/B/ST3/02955 of the National Science Centre,

Poland. The computations were partially performed at Poznań Supercomputing and Networking Center (PCSS).

References

- [1] L.D. Landau, E.M. Lifshitz, *Theory of Elasticity*, Pergamon Press, London, UK (1986).
- [2] R.F. Almgren, *An isotropic three-dimensional structure with Poisson's ratio = -1*, J. Elast. **15**, 427–430 (1985).
- [3] A.G. Kolpakov, *Determination of the average characteristics of elastic frameworks*, J. Appl. Math. Mech. **49**, 739–745 (1985).
- [4] R.S. Lakes, *Foam structures with a negative Poisson's ratio*, Science **235**, 1038–1040 (1987).
- [5] K.W. Wojciechowski, *Constant thermodynamic tension Monte Carlo studies of elastic properties of a two-dimensional system of hard cyclic hexamers*, Mol. Phys. **61**, 1247–1258 (1987).
- [6] K.W. Wojciechowski, *Two-dimensional isotropic model with a negative Poisson ratio*, Phys. Lett. A **137**, 60–64 (1989).
- [7] K.W. Wojciechowski, A.C. Brańka, *Negative Poisson ratio in a two-dimensional isotropic solid*, Phys. Rev. A **40**, 7222–7225 (1989).
- [8] K.W. Wojciechowski, *Non-chiral, molecular model of negative Poisson's ratio in two dimensions*, J. Phys. A: Math. Gen. **36**, 11765–11778 (2003).
- [9] K.E. Evans, *Auxetic polymers: a new range of materials*, Endeavour **15**, 170–174 (1991).
- [10] K.E. Evans, A. Alderson, *Auxetic materials: Functional materials and structures from lateral thinking!*, Adv. Mater. **12**, 617–628 (2000).
- [11] A. Alderson, K.L. Alderson, *Auxetic materials*, Proc. Inst. Mech. Eng. Part G-J. Aerosp. Eng. **221**, 565–575 (2007).
- [12] Y. Prawoto, *Seeing auxetic materials from the mechanics point of view: A structural review on the negative Poisson's ratio*, Comput. Mater. Sci. **58**, 140–153 (2012).
- [13] K.E. Evans, M.A. Nkansah, I.J. Hutchinson, S.C. Rogers, *Molecular network design*, Nature **353**, 124 (1991).
- [14] A.C. Brańka, D.M. Heyes, K.W. Wojciechowski, *Auxeticity of cubic materials under pressure*, Phys. Status Solidi B **248**, 96–104 (2011).
- [15] J. Schwerdtfeger, F. Wein, G. Leugering, R.F. Singer, C. Körner, M. Stingl, F. Schury, *Design of auxetic structures via mathematical optimization*, Adv. Mater. **23**, 2650–2654 (2011).
- [16] O. Duncan, T. Shepherd, C. Moroney, *Review of auxetic materials for sports applications: Expanding options in comfort and protection*, Applied Sciences **8**(6), 941 (2018).
- [17] T.-C. Lim, *Mechanics of Metamaterials with Negative Parameters*, Springer, Singapore (2020).
- [18] K. Alderson, S. Nazaré, A. Alderson, *Large-scale extrusion of auxetic polypropylene fibre*, Phys. Status Solidi B **253**(7), 1279–1287 (2016).
- [19] P. Verma, C.B. He, A.C. Griffin, *Implications for auxetic response in liquid crystalline polymers: X-ray scattering and space-filling molecular modeling*, Phys. Status Solidi B **257**(10), 2000261 (2020).
- [20] N. Novak, M. Vesenjajk, G. Kennedy, N. Thadhani, Z. Ren, *Response of chiral auxetic composite sandwich panel to fragment simulating projectile impact*, Phys. Status Solidi B **257**(10), 1900099 (2020).
- [21] F. Portone, M. Amorini, M. Montanari, R. Pinalli, A. Pedrini, R. Verucchi, R. Brighenti, E. Dalcanale, *Molecular auxetic polymer of intrinsic microporosity via conformational switching of a cavitand crosslinker*, Adv. Funct. Mater. **33**(51), 2307605 (2023).

- [22] T. Allen, T. Hewage, C. Newton-Mann, W. Wang, O. Duncan, A. Alderson, *Fabrication of auxetic foam sheets for sports applications*, *Phys. Status Solidi B* **254**(12), 1700596 (2017).
- [23] H.C. Cheng, F. Scarpa, T.H. Panzera, I. Farrow, H.-X. Peng, *Shear stiffness and energy absorption of auxetic open cell foams as sandwich cores*, *Phys. Status Solidi B* **256**(1), 1800411 (2019).
- [24] O. Duncan, F. Clegg, A. Essa, A.M.T. Bell, L. Foster, T. Allen, A. Alderson, *Effects of heat exposure and volumetric compression on Poisson's ratios, Young's moduli, and polymeric composition during thermo-mechanical conversion of auxetic open cell polyurethane foam*, *Phys. Status Solidi B* **256**(1), 1800393 (2019).
- [25] O. Duncan, A. Alderson, T. Allen, *Fabrication, characterization and analytical modeling of gradient auxetic closed cell foams*, *Smart Mater. Struct.* **30**(3), 035014 (2021).
- [26] F. Usta, F. Scarpa, H.S. Turkmen, P. Johnson, A.W. Perriman, Y.Y. Chen, *Multiphase lattice metamaterials with enhanced mechanical performance*, *Smart Mater. Struct.* **30**(2), 025014 (2021).
- [27] P. Verma, K.B. Wagner, A.C. Griffin, M.L. Shofner, *Reversibility of out-of-plane auxetic response in needle-punched nonwovens*, *Phys. Status Solidi B* **259**(12), 2200387 (2022).
- [28] A. Zulifqar, H. Hu, *Development of bi-stretch auxetic woven fabrics based on re-entrant hexagonal geometry*, *Phys. Status Solidi B* **256**(1), 1800172 (2019).
- [29] N. Jiang, H. Hu, *Auxetic yarn made with circular braiding technology*, *Phys. Status Solidi B* **256**(1), 1800168 (2019).
- [30] A. Zulifqar, T. Hua, H. Hu, *Single- and double-layered bistretch auxetic woven fabrics made of nonauxetic yarns based on foldable geometries*, *Phys. Status Solidi B* **257**(10), 1900156 (2020).
- [31] D. Tahir, M. Zhang, H. Hu, *Auxetic materials for personal protection: A review*, *Phys. Status Solidi B* **259**(12), 2200324 (2022).
- [32] J. Smardzewski, R. Klos, B. Fabisiak, *Design of small auxetic springs for furniture*, *Mater. Des.* **51**, 723–728 (2013).
- [33] T. Kuskun, A. Kasal, G. Caglayan, E. Ceylan, M. Bulca, J. Smardzewski, *Optimization of the cross-sectional geometry of auxetic dowels for furniture joints*, *Materials* **16**, 2838 (2023).
- [34] J. Kaufman, K. Farsad, A. Chinubhai, C. Bonsignore, R. Al-Hakim, *Auxetic stent increases venous inflow lumen in an ovine animal model*, *J. Vasc. Interv. Radiol.* **34**(3), S46–S47 (2023).
- [35] L. Meeusen, S. Candidori, L.L. Micoli, G. Guidi, T. Stanković, S. Graziosi, *Auxetic structures used in kinesiology tapes can improve form-fitting and personalization*, *Sci. Rep.* **12**, 13509 (2022).
- [36] M. Kapnisi, C. Mansfield, C. Marijon, A.G. Guex, F. Perbellini, I. Bardi, E.J. Humphrey, J.L. Puetzer, D. Mawad, D.C. Koutsogeorgis, D.J. Stuckey, C.M. Terracciano, S.E. Harding, M.M. Stevens, *Auxetic cardiac patches with tunable mechanical and conductive properties toward treating myocardial infarction*, *Adv. Funct. Mater.* **28**, 1800618 (2018).
- [37] X. Ren, J. Shen, T. Phuong, T. Ngo, Y.M. Xie, *Auxetic nail: Design and experimental study*, *Comp. Struct.* **184**, 288–298 (2018).
- [38] R.H. Baughman, J.M. Shacklette, A.A. Zakhidov, S. Stafstrom, *Negative Poisson's ratios as a common feature of cubic metals*, *Nature* **392**, 362–365 (1998).
- [39] J.W. Narojczyk, M. Kowalik, K.W. Wojciechowski, *Influence of nanochannels on Poisson's ratio of degenerate crystal of hard dimers*, *Phys. Status Solidi B* **253**, 1324–1330 (2016).
- [40] P.M. Piglowski, J.W. Narojczyk, K.W. Wojciechowski, K.V. Tretiakov, *Auxeticity enhancement due to size polydispersity in fcc crystals of hard-core repulsive Yukawa particles*, *Soft Matter* **13**, 7916–7921 (2017).
- [41] K.V. Tretiakov, P.M. Piglowski, J.W. Narojczyk, K.W. Wojciechowski, *Selective enhancement of auxeticity through changing a diameter of nanochannels in Yukawa systems*, *Smart Mater. Struct.* **27**, 115021 (2018).
- [42] K.V. Tretiakov, P.M. Piglowski, J.W. Narojczyk, M. Bilski, K.W. Wojciechowski, *High partial auxeticity induced by nanochannels in [111]-direction in a simple model with Yukawa interactions*, *Materials* **11**, 2550 (2018).
- [43] J.W. Narojczyk, K.W. Wojciechowski, K.V. Tretiakov, J. Smardzewski, F. Scarpa, P.M. Piglowski, M. Kowalik, A.R. Imre, M. Bilski, *Auxetic properties of a f.c.c. crystal of hard spheres with an array of [001]-nanochannels filled by hard spheres of another diameter*, *Phys. Status Solidi B* **256**, 1800611 (2019).
- [44] J.W. Narojczyk, K.W. Wojciechowski, *Poisson's ratio of the f.c.c. hard sphere crystals with periodically stacked (001)-nanolayers of hard spheres of another diameter*, *Materials* **12**, 700 (2019).
- [45] J.W. Narojczyk, K.W. Wojciechowski, J. Smardzewski, A.R. Imre, J.N. Grima, M. Bilski, *Cancellation of auxetic properties in f.c.c. hard sphere crystals by hybrid layer-channel nano-inclusions filled by hard spheres of another diameter*, *Materials* **14**, 3008 (2021).
- [46] J.W. Narojczyk, K.W. Wojciechowski, J. Smardzewski, K.V. Tretiakov, *Auxeticity tuning by nanolayer inclusion ordering in hard sphere crystals*, *Materials* **17**, 4564 (2024).
- [47] J.W. Narojczyk, J. Smardzewski, P. Kedziora, K.V. Tretiakov, K.W. Wojciechowski, *Fine-tuning of elastic properties by modifying ordering of parallel nanolayer inclusions in hard sphere crystals*, *Phys. Status Solidi B* **261**, 2400529 (2024).
- [48] R. Ali, M.R. Saleem, M. Roussey, J. Turunen, S. Honkanen, *Fabrication of buried nanostructures by atomic layer deposition*, *Sci. Rep.* **8**, 15098 (2018).
- [49] K.W. Wojciechowski, K.V. Tretiakov, M. Kowalik, *Elastic properties of dense solid phases of hard cyclic pentamers and heptamers in two dimensions*, *Phys. Rev. E* **67**, 036121 (2003).
- [50] D. Frenkel, *Order through entropy*, *Nat. Mater.* **14**, 9–12 (2015).
- [51] K.V. Tretiakov, K.W. Wojciechowski, *Auxetic, partially auxetic, and nonauxetic behaviour in 2D crystals of hard cyclic tetramers*, *Phys. Status Solidi RRL* **14**, 2000198 (2020).
- [52] J.P. Hansen, I.R. McDonald, *Theory of Simple Liquids*, Academic Press, Amsterdam, Netherlands, 2006.
- [53] K.W. Wojciechowski, *Poisson's ratio of anisotropic systems*, *Comput. Methods Sci. Technol.* **11**(1), 73–79 (2005).
- [54] M. Parrinello, A. Rahman, *Polymorphic transitions in single crystals: A new molecular dynamics method*, *J. Appl. Phys.* **52**, 7182–7190 (1981).
- [55] M. Parrinello, A. Rahman, *Strain fluctuations and elastic constants*, *J. Chem. Phys.* **76**, 2662–2666 (1982).
- [56] J.H. Weiner, *Statistical Mechanics of Elasticity*, Wiley, New York, USA, 1983.
- [57] S.P. Tokmakova, *Stereographic projections of Poisson's ratio in auxetic crystals*, *Phys. Status Solidi B* **242**(3), 721–729 (2005).
- [58] J.F. Nye, *Physical Properties of Crystals: Their Representation by Tensors and Matrices*, Clarendon Press, Oxford, UK (1957).



Jakub W. Narojczyk received his PhD from the Institute of Molecular Physics of the Polish Academy of Sciences (IMP PAS) in Poznań. Recently he received habilitation from IMP PAS for his work on elastic properties of hard sphere models. He is a computational physicist with a strong background in Monte Carlo and Molecular Dynamics simulation methods. He has in-depth knowledge of C programming language and a solid experience in administration of GNU/Linux class operating systems as well as High-Performance Computing environment. He works as an Assistant Professor in the IMP PAS, where he conducts research (by means of computer simulations) on elastic properties of model materials, with emphasis on their Poisson's ratio. The research is aimed at the search for systems for which the Poisson's ratio takes negative values (such materials are called auxetics) as well as mechanisms and phenomena responsible for the decrease of the Poisson's ratio of materials. Currently, his studies are focused on the influence of various forms of nanoinclusions in the atomic structure on the elastic properties of various model systems. He guest co-edited one special issue of *Physica Status Solidi B* and four abstract books from the conferences on Auxetics and Related Systems. He is a peer reviewer for various scientific journals including *Applied Physics Letters*, *Applied Sciences*, *Advanced Theory and Simulations*, *Carbon*, *Materials and Design*, *Physica Status Solidi B*, and *Computational Methods in Science and Technology*.



Krzysztof Witold Wojciechowski is a Full Professor at the Institute of Molecular Physics of the Polish Academy of Sciences (IMP PAS) in Poznań. He is also a Full Professor at the President Stanisław Wojciechowski University in Kalisz. He received the MSc degree in Theoretical Physics and the MSc degree in Mathematics from the Adam Mickiewicz University in Poznan. He earned the PhD in Physics from the IMP PAS, where he also habilitated. His research interests concern, among other topics, statistical-mechanics of hard-body systems, algorithms for simulations of many-body systems, auxetics and influence of various mechanisms on the Poisson's ratio of condensed matter systems, materials with unstable inclusions, generators of (pseudo)random numbers, applications of fractional derivative in physics, and exotic liquid crystalline phases. He is an author and co-author of more than 200 research papers written in English, Polish or Russian and published in such journals as *Phys. Rev. Lett.*, *Advanced Materials*, *Phys. Lett. A*, *Phys. Rev. A*, *Phys. Rev. B*, *Phys. Rev. E*, *J. Chem. Phys.*, *J. Phys. Chem. A*, *Molecular Physics*, etc. Prof. Wojciechowski guest co-edited more than two dozen thematic issues (on auxetics and related materials, mechanics of continuous media, statistical mechanics of condensed matter, computer simulation methods, nonlinear and disordered systems) for international journals including *Phys. Status Solidi B* (15), *J. Non-Cryst. Solids* (4), *Smart Materials and Structures* (2), *J. Mech. Mat. Struct.* (2), *Rev. Adv. Mat. Sci.* (2), etc. He is a member of the Editorial Board of the CMST (OWN Poznań), *Smart Materials and Structures* (IOP Publishing), and *TASK Quarterly* (TASK).